JOURNAL OF SOLID STATE CHEMISTRY 137, 218–222 (1998)
ARTICLE NO. SC977704

# Sc–Sc Bonding in the New Ternary Phosphide ScNiP

Holger Kleinke and Hugo F. Franzen

*Ames Laboratory—U.S. Department of Energy, Iowa State University, Ames, Iowa 50011*

Received June 11, 1997; accepted November 14, 1997

**The new phosphide ScNip can be synthesized by arc-melting of ScP and Ni, or by arc-melting of Sc with NiP. The lattice constants, as obtained from the bulk sample, are $a = 6.3343(8)$ Å, $b = 3.7375(7)$ Å, $c = 7.0917(8)$, and $V = 167.89(4)$ Å$^3$. ScNiP crystallizes in the $Co_2Si$ structure type. Although one might assign the trivalent state to Sc, corresponding to a formal ionic formula of $Sc^{3+}Ni^{\pm 0}P^{3-}$, the structure of ScNiP contains Sc–Sc bonds and shows weak metallic properties, as expected based on extended Hückel calculations.** © 1998 Academic Press

***Key Words*: Scandium nickel phosphide; preparation; structure and bonding; pseudo gap; magnetism.**

## INTRODUCTION

Within the past two years, 12 new metal-rich ternary phosphides have been uncovered using the early transition metal atoms $M$ = Zr, Hf, and the iron-group metal atoms $M'$ = Fe, Co, and Ni. A common feature in the structures of the Zr or Hf rich phosphides is that the $M'$ and P atoms are both situated in (capped) trigonal prisms formed by the $M$ atoms, which build up a three-dimensional network. This is true for the structures of $Zr_9Ni_2P_4$ (1), $M_2M'P$ (2, 3), $Hf_5Co_{1+x}P_{3-x}$ (4), and $Hf_5Ni_{1+x}P_3$ (5), and in all these structures, strong bonding character is observed for the $M$–P, $M'$–P, $M$–$M$, and $M$–$M'$ interactions. The two different kinds of metal–metal bonds, $M$–$M$ and $M$–$M'$ interactions, contribute significantly to the stability of these refractory materials.

No comparable compounds are known so far for the group 3 elements. In general, the question is, are the metal atoms Sc, Y, and La, despite the lower electron counts compared to Zr and Hf, and in the case of Sc the relatively small 3*d* orbitals, capable of forming similar pnictides which contain $M$–$M$ bonds. The highest Sc content (33.3 at.%) has been found in ScCoP, which was prepared using a tin flux. As determined by powder diffraction, ScCoP occurs in the $Co_2Si$ structure type (6). Here we report on the isostructural ScNiP. We discuss the bonding and physical properties as well as reasons for the nonexistence of a "ScFeP."

## EXPERIMENTAL

### *Synthesis*

Because of the high vapor pressure of elemental phosphorus the reactants did not include phosphorus in its elemental form, but consisted of the phosphides and elemental metals. All phosphides used, i.e., ScP, FeP, CoP, and NiP, were prepared from mixtures of the elements in the stoichiometric ratio of 1 : 1 in sealed silica tubes at 800 °C in a resistance furnace. The starting elements were obtained from Alfa or Fisher (Fe: Alfa, powder, −22 mesh, 99.999%; Co: Alfa, powder, −50 + 150 mesh, 99.9%; Ni: Fisher, powder, purified; P: Alfa, powder, −100 mesh, red amorphous, 99%).

ScCoP and ScNiP were synthesized by arc-melting of pressed pellets of ScP and Co and Ni, respectively, under a dynamic Argon flow. Analogous melting of ScP with Fe or Sc with FeP both yielded ScP and Fe as main products. No reflections of a "ScFeP," isotypic to ScCoP and ScNiP, were found in the experimentally obtained powder diagrams.

In contrast, the powder diagrams of ScCoP and ScNiP could be indexed based on orthorhombic symmetry, using the Guinier technique with silicon as internal standard and Cu$K\alpha$ radiation. The ideal lattice constants are listed in Table 1. Our results for the cell dimensions of ScCoP are in agreement with those given by Jeitschko *et al.* (6). The volume of the unit cell of ScNiP is significantly greater than that of ScCoP, despite the smaller Pauling radius of Ni ($r_{Ni} = 1.154$ Å $< r_{Co} = 1.162$ Å (7)) .

In order to obtain single crystals suitable for a single crystal structure investigation, the arc-melted sample containing ScNiP was annealed in an induction furnace under a dynamic vacuum of $\approx 2 \times 10^{-6}$ mbar at a maximum temperature of 1350°C over a period of 5 h.

### *Structure Determination*

A needle-like single crystal from the annealed ScNiP sample was selected for the structure determination. A four-circle diffractometer with a rotating anode was used for the data collection (RIGAKU AFC6R, Mo$K\alpha$). The cell



0022-4596/98 $25.00

**TABLE 1**

| Compound | $a$/Å | $b$/Å | $c$/Å | $V$/Å$^3$ |
|---|---|---|---|---|
| ScCoP[a] | 6.2706(8) | 3.7479(6) | 7.054(1) | 165.79(4) |
| ScCoP[b] | 6.268(2) | 3.750(1) | 7.050(3) | 165.7 |
| ScNiP | 6.3343(8) | 3.7375(7) | 7.0917(8) | 167.89(4) |

[a] This work.
[b] Ref. (6).

constants were refined using the setting angles of 19 carefully centered reflections in the range of $16.89^\circ < 2\theta < 21.95^\circ$. The data were corrected for Lorentz and polarization effects. Two octants were measured and later merged. An empirical absorption correction ($\Psi$ scan) was applied.

The systematic extinctions ($k + l = 2n + 1$ for all $0kl$ and $h = 2n + 1$ for all $hk0$ reflections) restricted the possible space groups to $Pnma$ or $Pna2_1$. The structure model, as obtained from the direct methods (SHELXS (8)), could be refined in the higher symmetry ($Pnma$). Reducing the symmetry by removing the mirror plane ($Pnma \rightarrow Pna2_1$) neither improved the residual factors nor resulted in any significant changes of the structure model. All structure refinements were performed using the TEXSAN program package (9). Refinements against $F^2$ with anisotropic temperature factors for all sites converged quickly to $R(F^2) = 0.061, R_w(F^2) = 0.064$, goodness of fit $= 1.09$ ($R(F) = 0.036$). More crystallographic details are listed in Table 2, atomic positions and temperature factors in Table 3, and selected bond distances for ScNiP in Table 4.

**TABLE 2**
**Selected Crystallographic Data for ScNiP**

| | |
|---|---|
| Empirical formula | ScNiP |
| Molecular weight | 134.63 g/mol |
| Temperature of data collection | 295 K |
| Crystal dimensions | 0.06 mm × 0.002 mm × 0.001 mm |
| Space group | $Pnma$ (No. 62) |
| Unit cell dimensions | $a = 6.327(2)$ Å, $b = 3.728(2)$ Å, $c = 7.081(3)$ Å, $V = 167.0(2)$ Å$^3$ |
| Number of formula units | 4 |
| Calculated density | 5.353 g/cm$^3$ |
| Absorption coefficient | 15.76 mm$^{-1}$ |
| $F(000)$ | 256 |
| Scan mode, scan width | $\omega$–$2\theta$, $(1.26 + 0.34\tan\theta)^\circ$ |
| Scan speed | 4.0°/min (in $\omega$, 3 rescans) |
| Range of $2\theta$ | 4°–60° |
| No. of measured reflections | 571 |
| No. of independent reflections | 324 ($R_{int} = 0.114$) |
| No. of observed reflections ($I > 3\sigma(I)$) | 138 |
| No. of parameters refined | 20 |
| $R(F^2)$, $R_w(F^2)$, goodness of fit | 0.061, 0.064, 1.09 |
| Extinction coefficient | $0.25705 \times 10^{-5}$ |
| Max., min. peak in final diff. map | 1.29 $e^-$/Å$^3$, $-1.64$ $e^-$/Å$^3$ |
| Absorption correction | $\Psi$ scan |
| Min., max. transmission | 0.73, 0.99 |

**TABLE 3**
**Atomic Positions and Temperature Factors [Å$^2$] for ScNiP[a]**

| Atom | $x$ | $z$ | $B_{eq}$/Å$^b$ | $U_{11}$/Å$^2$ | $U_{22}$/Å$^2$ | $U_{33}$/Å$^2$ | $U_{13}$/Å$^2$ |
|---|---|---|---|---|---|---|---|
| Sc | 0.0221(4) | 0.6853(3) | 0.4(1) | 0.005(1) | 0.003(1) | 0.005(1) | −0.000(1) |
| Ni | 0.1423(3) | 0.0619(2) | 0.51(7) | 0.009(1) | 0.0049(9) | 0.0057(8) | 0.0016(7) |
| P | 0.2653(5) | 0.3813(4) | 0.3(1) | 0.004(1) | 0.003(2) | 0.005(1) | 0.001(1) |

[a] All atoms on Wyckoff position 4$c$, $y = 1/4$, $U_{12} = U_{23} = 0$.
[b] $B_{eq} = (8\pi^2/3)\sum_i\sum_j U_{ij} a_i^* a_j^* \mathbf{a}_i\mathbf{a}_j$.

*Magnetic Properties*

Magnetic data were obtained for the annealed bulk sample of ScNiP (37.3 mg). Temperature dependent measurements were made at 3 Tesla in the temperature range of 6–297 K on a Quantum Design MPMS SQUID magnetometer. The data were corrected for the diamagnetic atom cores.

## RESULTS AND DISCUSSION

ScNiP is isotypic to Ti$M'$P ($M'$ = Fe, Co, Ni) (10, 11), Zr$M'$P ($M'$ = Fe, Co) (10, 12), and Hf$M'$P ($M'$ = Fe, Co, Ni), whereas ZrNiP occurs in the $Ni_2In$ structure type (13). The structure of ScNiP can be described based on the trigonal prisms around the P atoms, which are interconnected via common edges to form puckered sheets parallel to [100], as emphasized via thick lines in Fig. 1. The Sc atoms form four corners and one cap, and the Co atoms form two corners and two caps of each trigonal prism. The sheets of prisms are directly connected to form a three-dimensional network, because the caps of the prisms of one sheet form the corners of the prisms of the neighboring sheet.

The structure of ScNiP can also be described based on the coordination polyhedra around the metal atoms. It consists of edge-condensed (distorted) square $ScP_5$ pyramids, with the Ni atoms in tetrahedral voids of the P sublattice (Fig. 2). One further P atom, situated at a much larger distance from

**TABLE 4**
**Selected Interatomic Distances [Å] < 3.8 Å for ScNiP**

| Central atom | Neighbor | Distance | No. | Central atom | Neighbor | Distance | No. |
|---|---|---|---|---|---|---|---|
| Sc | Sc | 3.232(4) | 2× | Ni | Sc | 2.773(3) | |
| Sc | Sc | 3.293(2) | 2× | Ni | Sc | 2.786(2) | 2× |
| Sc | Sc | 3.729(2) | 2× | Ni | Sc | 2.958(2) | 2× |
| Sc | Ni | 2.773(3) | | Ni | Sc | 2.973(3) | |
| Sc | Ni | 2.786(2) | 2× | Ni | Ni | 2.736(3) | 2× |
| Sc | Ni | 2.958(2) | 2× | Ni | Ni | 3.729(2) | 2× |
| Sc | Ni | 2.973(3) | | Ni | P | 2.335(2) | 2× |
| Sc | P | 2.646(4) | | Ni | P | 2.391(4) | |
| Sc | P | 2.647(3) | 2× | Ni | P | 2.419(4) | |
| Sc | P | 2.685(3) | 2× | | | | |
| Sc | P | 3.472(4) | | | | | |

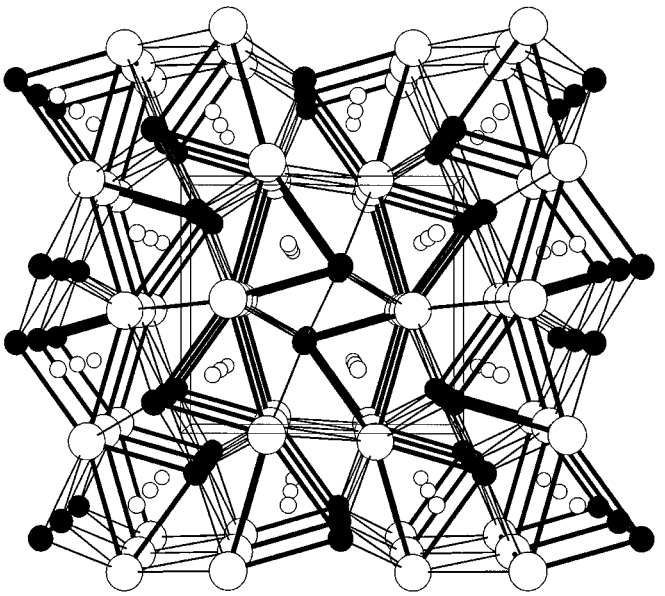

**FIG. 1.** Structure of ScNiP in a projection along [010]. Small, black circles: P; medium, white: P; large, white: Sc atoms. Horizontal: *c* axis. Only metal–metal bonds are shown.

the central Sc atom (3.472(4) Å, compared to the five other Sc–P distances between 2.646(4) Å and 2.685(3) Å), completes the Sc coordination sphere to a strongly distorted octahedron. A calculation of the Pauling bond orders, using Pauling's equation $d(n) = d(1) - 0.6 \log n$, with $n$ = bond order, $r_{Sc} = 1.439$ Å and $r_P = 1.100$ Å (7), shows that the Sc–P interactions $< 2.7$ Å should have bonding character with Pauling bond orders between 0.66 and 0.57, as expected based on the facts that Sc is the most electropositive and P the most electronegative element in ScNiP. On the other hand, the bond order of the long Sc–P distance of 3.472(4) Å (0.04) is rather small. The Ni–P distances, being the shortest interatomic separations in this structure, also have significant bond orders (ranging from 0.73 for $r_{Ni-P} = 2.335(2)$ Å to 0.53 for $r_{Ni-P} = 2.419(4)$ Å).

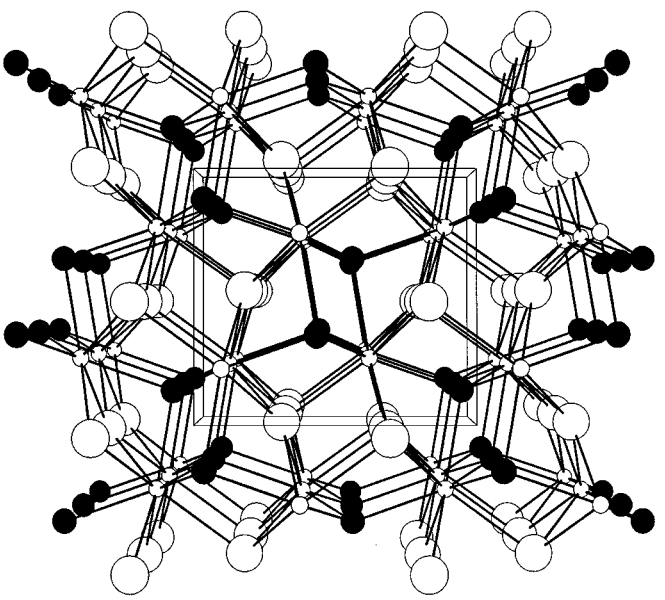

**FIG. 2.** Structure of ScNiP in a projection along [010]. Small, black circles: Co; medium, white: P; large, white: Sc atoms. Horizontal: *c* axis. Only metal–P bonds are shown.

Besides Sc–P and Ni–P bonds, there are also relatively short Sc–Sc, Sc–Ni, and Ni–Ni interactions between adjacent layers of trigonal $Sc_4Ni_2P$ prisms. The Ni–Ni distance between the prisms of 2.736(3) Å is much shorter than that within the prism (3.729(2) Å). Similarly, the shortest Sc–Sc interaction (3.232(4) Å) is found between two $Sc_4Ni_2P$ prisms, whereas the shortest one within a $Sc_4Ni_2P$ prism is slightly longer (3.293(2) Å). However, the relatively shortest metal–metal bonds in ScNiP, i.e., those with the highest bond order, are those between Sc and Ni. We calculated the Pauling bond orders of all the different metal–metal bonds for a first estimation of the bond strengths of the different metal–metal bonds. The highest Pauling bond order (0.51) is calculated for the Sc–Ni bond of 2.773(3) Å, the other Sc–Ni bond orders of 0.48, 0.25, and 0.23 are also a hint of the occurrence of Sc–Ni bonding. This bonding corresponds to the Lewis acid/base concept, considering the electron-poor metal Sc as the acid and the electron-rich metal Ni as the base. However, the two Sc–Sc distances $< 3.3$ Å also have significant bond orders of 0.26 and 0.20, respectively. It is concluded, based on these values, that a significant electron density at the Sc atoms is available for a positive overlap population between the Sc atoms, because otherwise a repulsive Coulomb interaction would preclude such a close distance.

In order to further investigate the character of the different metal–metal interactions, we calculated the electronic structure of ScNiP using the extended Hückel approximation. We performed a charge iteration on the metal atoms in ScNiP, taking the P parameters from standard sources (14). The charge-consistent metal parameters as well as the P parameters can be found in Table 5.

To a first approximation, the density of states of ScNiP consists of three parts in the energy window shown in Fig. 3 (between $-16$ eV and $-8$ eV). Below this energy window, the 3*s* states of P occur, and at higher energies the 3*p* orbitals of P (between $-16$ eV and $-12.5$ eV) predominate. Between these states and the next peak, which has mainly Ni *d* and also via covalent mixing some Sc *d* character, is a significant gap. The sharp Ni peak overlaps only slightly with the much broader Sc *d* orbitals exactly at the Fermi level of $-9.97$ eV. As a consequence, the Fermi level lies in a pseudo gap, i.e., only a very small number of states is found at the Fermi level. Thus, weak metallic properties can be assumed.

**TABLE 5**
**Parameters Used for the EH Calculations**

| Orbital | $H_{ii}$/eV | $\varsigma_1$ | $c_1$ | $\varsigma_2$ | $c_2$ |
|---|---|---|---|---|---|
| Sc, 4*s* | − 9.00 | 1.30 | | | |
| Sc, 4*p* | − 4.32 | 1.30 | | | |
| Sc, 3*d* | − 9.42 | 4.35 | 0.4228 | 1.70 | 0.7276 |
| Ni, 4*s* | − 8.67 | 1.93 | | | |
| Ni, 4*p* | − 4.20 | 1.93 | | | |
| Ni, 3*d* | − 11.06 | 5.75 | 0.5862 | 2.200 | 0.5845 |
| P, 3*s* | − 18.60 | 1.88 | | | |
| P, 3*p* | − 12.50 | 1.63 | | | |

In an attempt to confirm the metallic character of ScNiP, we measured the magnetic susceptibilities between 6 K and 297 K of the annealed bulk sample of ScNiP. Figure 4 shows the magnetic susceptibility (circles) as a function of the temperature. The small value of the magnetic susceptibility of room temperature of $9.1 \times 10^{-5}$ emu/mol suggests Pauli paramagnetism. The increase of the magnetic signal at lower temperature points to a paramagnetic impurity, following the Curie-Weiss law $\chi_{\text{para}} = C/(T - \theta)$. With this supposition, the raw data have been fitted to the equation $\chi_{\text{obs}} = \chi_{\text{para}} + \chi$, with $\chi_{\text{obs}}$ = observed molar susceptibility and $\chi$ = molar susceptibility of ScNiP. According to this fit, the Curie-Weiss constant is determined to $C = 1.22 \times 10^{-3}$ emu $\text{mol}^{-1}K$, and $\theta = -9.716\,K$, and the impurity is estimated to be 5.7 at.% for a compound with a total spin magnetic moment of $S = 1/2$, corresponding to one unpaired localized electron per formula unit. The temperature dependent contribution of the Curie-Weiss impurity is shown as crosses in Fig. 4. The resulting values for $\chi$, shown as diamonds in Fig. 4, are basically temperature independent, which confirms the validity of the fitting equation used. The so corrected susceptibility at room temperature of $8.66 \times 10^{-5}$ emu/mol, is almost equal to the susceptibility as measured and corrected for the diamagnetic cores ($9.1 \times 10^{-5}$ emu/mol). These small positive values are typical for Pauli paramagnetic compounds, which means that there are some itinerant electrons present. Since the magnetic susceptibility of a Pauli paramagnet is proportional to the density of states at the Fermi level, we conclude that there is a small, but significant, density of states at the Fermi level as calculated using the extended Hückel approximation, and that the metallic character of ScNiP is confirmed by our experiment.

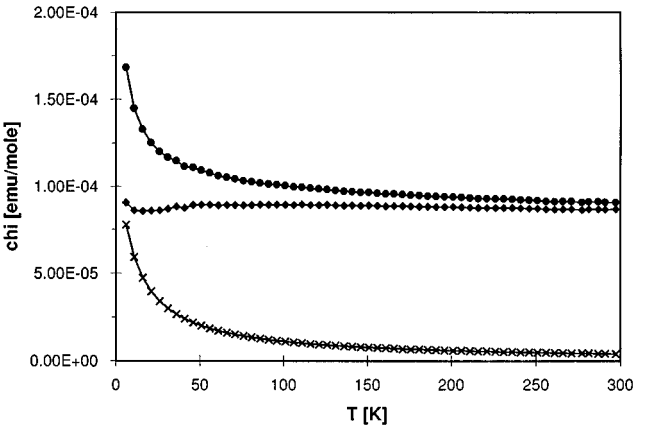


**FIG. 4.** Temperature dependence of the magnetic susceptibilities for ScNiP. Circles: raw data after the diamagnetic core correction; crosses: fit of the paramagnetic impurity; diamonds: difference between raw data and the contribution of the paramagnetic impurity.

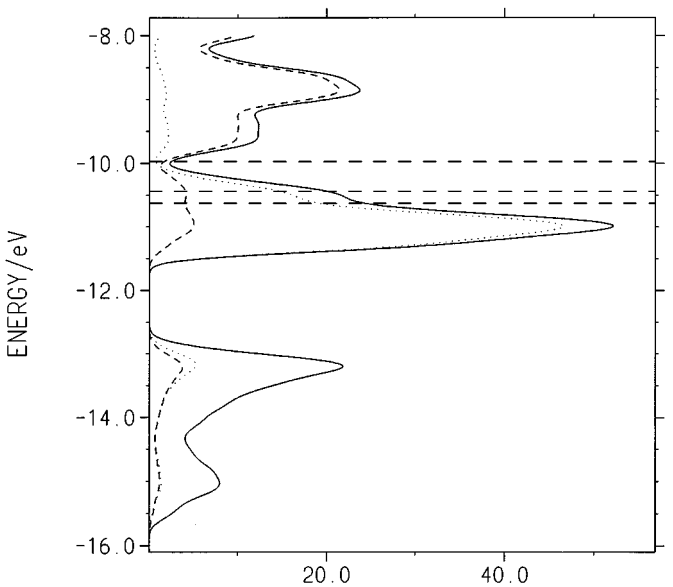


**FIG. 3.** Densities of states for ScNiP. Dashed horizontal lines: Fermi levels for $vec = 64\,e^-$, $vec = 68\,e^-$ and $vec = 72\,e^-$, respectively (from bottom to top). Solid line: total DOS; dashed: Sc; dotted line: Ni contributions.

The assignment of the different peaks discussed above points to filled 3*s* and 3*p* states of P and also to filled Ni *d* states, which corresponds to a formal ionic formula of $Sc^{3+}Ni^{\pm 0}P^{3-}$. However, the significant Sc contributions to the peaks in the DOS below the Fermi level, caused by covalent mixing of the Sc states with the Ni, as well as the P states, prove that Sc is not fully oxidized to $Sc^{3+}$. This enables Sc to form the observed Sc–Sc bonds. This supposition is confirmed by the calculated crystal orbital overlap populations, as shown in Fig. 5. The Sc–Sc interactions (solid line in Fig. 5) have bonding character between $-16\,eV$ and $-9\,eV$. The Fermi level of ScNiP lies just below a region where many bonding Sc–Sc states occur, which means that raising the Fermi level would result in stronger Sc–Sc bonding.

Figure 5 also shows the Sc–Ni (short dashes), Sc–P (long dashes), Ni–Ni (dash-dotted line), and Ni–P (dotted line) interactions. Each of these interactions is summed up to

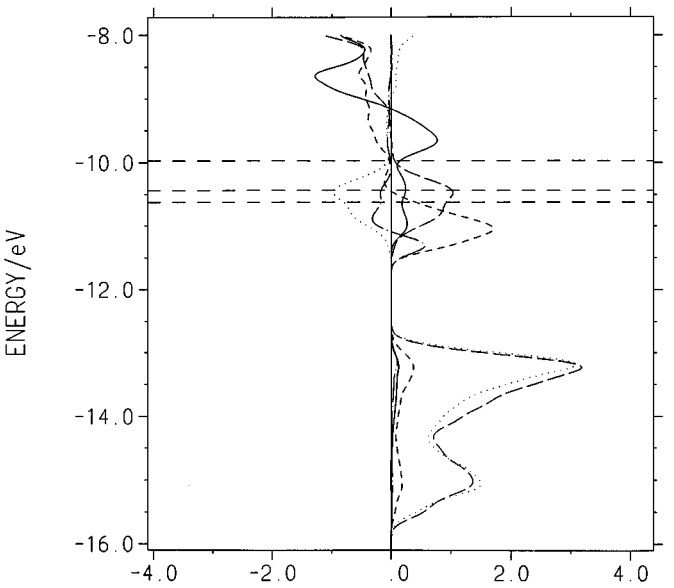


**FIG. 5.** Summed crystal orbital overlap populations for ScNiP. Horizontal lines: Fermi levels for $vec = 64\,e^-$, $vec = 68\,e^-$, and $vec = 72\,e^-$, respectively (from bottom to top). Left: antibonding; right: bonding. Solid line: Sc–Sc; dashed line: Sc–Ni; long dashes: Sc–P; dashed-dotted line: Ni–Ni; dotted line: Ni–P interactions.

bonding character, but some antibonding Ni–P, Ni–Ni, and Sc–Ni states are filled at the Fermi level of ScNiP. From these results, it is not obvious why an isostructural "ScFeP" did not form in our experiments. A (theoretical) substitution of Ni by Co or Fe would yield a lower valence electron concentration and thus lower lying Fermi levels as indicated by the horizontal dashed lines in Fig. 5. Going from ScNiP to hypothetical "ScFeP," the bonding character of the Sc–Sc and Sc–P bonds decreases, whereas on the other hand the bonding character of the $M'$–$M'$ and $M'$–P increases because fewer antibonding states are filled. Intuitively, one concludes that a structure type like $Co_2Si$ with short Sc–Sc bonds is not favored for compounds with a low electron count. A comparison with the related Ti–$M'$–P system underlines this supposition, because TiMnP, being isoelectronic with the hypothetical "ScFeP," is found to form the $Fe_2P$ structure type (15).

However, ScCoP does crystallize in the same structure type as ScNiP. Although the radius of nickel is smaller than that of cobalt (1.154 Å vs 1.162 Å), the unit cell of ScNiP is larger than the cell of ScCoP. This can be understood based on the filling of antibonding Sc–$M'$, $M'$–$M'$, and $M'$–P states when Co is replaced by Ni. The fact, that the $b$ axis of ScNiP is smaller than the ScCoP $b$ axis, is explained by the occurrence of (weak) Sc–Sc bonds parallel to [010], which are stronger in case of ScNiP. The above mentioned Sc–$M'$, $M'$–$M'$, and $M'$–P are not parallel to [010] and lie partly in the $ac$-plane so that their influence is largest on the $a$ and $c$ axes.

## ACKNOWLEDGMENTS

H.K. thanks the DFG for the financial support of this work. The Ames Laboratory is operated by Iowa State University for the U.S. Department of Energy under Contract W-7405-Eng-82 and is part of the Institute for Physical Research and Technology consortium of fundamental and applied research centers.

## REFERENCES

1. H. Kleinke and H. F. Franzen, *Inorg. Chem.* **35,** 5272 (1996).
2. H. Kleinke and H. F. Franzen, *Angew. Chem., Int. Ed. Engl.* **36,** 513 (1997).
3. H. Kleinke and H. F. Franzen, *J. Solid State Chem.* **131,** 379 (1997).
4. H. Kleinke and H. F. Franzen, *J. Alloys Comp.* **238,** 68 (1996).
5. H. Kleinke and H. F. Franzen, *Chem. Mater.* **9,** 1030 (1997).
6. W. Jeitschko and E. J. Reinbold, *Z. Naturforsch.* **40b,** 900 (1985).
7. L. Pauling, "The Nature of the Chemical Bond," 3rd ed., Cornell Univ. Press, Ithaca, NY, 1948.
8. G. M. Sheldrick, "SHELXS-86," Universität Göttingen, Germany.
9. TEXSAN, "Single Crystal Structure Analysis Software, Version 5.0," Molecular Structure Corp., The Woodlands, TX, 1989.
10. S. Rundqvist and P. C. Nawapong, *Acta Chem. Scand.* **20,** 2250 (1966).
11. S. V. Muchnik, Y. F. Lomnitskaya, V. B. Chernogorenko, and K. A. Lynchak, *Sov. Powd. Met. Met. Ceram.* **28,** 138 (1989).
12. N. Chaichit, P. Chalugune, S. Rukvichai, P. Choosang, V. Kaewchansilp, C.-A. Pontchour, P. Phavanantha, and S. Pramatus, *Acta Chem. Scand.* **A32,** 309 (1978).
13. H. Kleinke and H. F. Franzen, *Z. Anorg. Allg. Chem.* **622,** 1893 (1996).
14. E. Clementi and C. Roetti, *Atomic Data and Nuclear Data Tables* **14,** 177 (1974).
15. R. Montreuil, B. Deyris, A. Michel, A. Rouault, P. l'Héritier, A. Nylund, J. P. Sénateur, and R. Truchart, *Mater. Res. Bull.* **7,** 813 (1972).